An Experimental and Theoretical Investigation of the Carbon Dioxide Insertion Process into the Tungsten−Nitrogen Bond of an Anionic W(0) Complex

Donald J. Darensbourg,* Brian J. Frost, and David L. Larkins

Department of Chemistry, Texas A&M University, P.O. Box 30012, College Station, Texas 77842

Received September 5, 2000

The pyridine bound 2-aminopyridine (2APH) derivative of tungsten pentacarbonyl has been prepared from photogenerated $W(CO)_5THF$ and 2APH. Deprotonation of the distal amine group by sodium hydride has provided two complexes, $[Na][W(CO)_5(2AP)]$ and $[Na]_2[W(CO)_4(2AP)]_2$. Both complexes have been characterized by X-ray crystallography with the monomeric derivative being crystallized as its $[Na_2(18\text{-crown-}6)][W(CO)_5(2AP)]_2$ salt which exhibits strong $Na^+\cdots{}^-NH$ interactions. Photolysis of $W(CO)_6$ in the presence of excess 2-aminopyridine in THF has led to an efficient synthesis of the chelated neutral derivative, $W(CO)_4(2APH)\cdot 2APH$, where the extra equivalent of 2APH is hydrogen bonded to its bound counterpart. The 2-aminopyridine molecule of solvation was almost quantitatively removed via aqueous washings. Deprotonation of $W(CO)_4(2APH)$ with NaH afforded the amidopyridine derivative which was shown to rapidly undergo reaction with CO_2 to yield the chelated carbamate complex, $W(CO)_4(OC(O)2AP)^-$. Nevertheless, because of the presence of small quantities of free 2-aminopyridine during the reactions with CO_2, we have not been able to conclusively rule out participation by a ligand substitution process involving $NC_5H_4NHCOOH$. Ab initio computations were found to substantiate many of these experimental observations. That is, in the monodentate bound $W(CO)_5(2APH)$ derivative, binding through the pyridine nitrogen atom is favored by about 29 kJ/mol over the amine nitrogen atom, whereas the opposite site for binding is preferred for the deprotonated amido analogue, $W(CO)_5(2AP)^-$. Furthermore, both forms of $W(CO)_5(2AP)^-$ were found to be more stable than the chelated tungsten tetracarbonyl anion plus CO. On the other hand, CO_2 insertion into the $W(CO)_4(2AP)^-$ anion to provide the chelated carbamate, $W(CO)_4(OC(O)2AP)^-$, was thermodynamically favored by >110 kJ/mol. Finally, both experimental and theoretical studies were inconclusive with regard to identifying reaction intermediates during the CO_2 insertion pathway which involve prior interactions of CO_2 at the amido nitrogen center.

Introduction

Metal carbamates, which are ostensibly the products of CO_2 insertion into a metal-amide bond, are relevant to several synthetic and metallobiochemical processes. For example, the metal mediated preparation of N,N′-dialkylureas and urethanes from amines and CO_2 likely involve metal coordinated nitrogen reaction at the carbon of CO_2.[1−3] Similarly, the ribulose 1,5-bisphosphate carboxylase(Rubisco) enzyme, which is responsible for the initial step in the fixation of CO_2 by plants via photosynthesis, has been shown to contain a carbamalated lysine at the active site.[4,5] Other enzymes which contain carbamate linkages at the active site include biotin-dependent carboxylases[6,7] and nickel urease.[8]

The importance of the reaction depicted in eq 1 notwithstanding, limited mechanistic information regarding this process has appeared in the literature. Related to this issue Chisholm and co-workers have investigated CO_2 insertions into M−N bonds in high oxidation state metal amides.[9,10] These researchers noted that these reactions were accelerated by free amines and concluded that CO_2 does not formally insert into a metal-nitrogen bond but by a ligand exchange process as described below in eqs 2 and 3. Consistent with this proposal the process was found to be catalytic in free amine. Indeed, the facile nature of reaction 2 is one of the major caveats in studying the mechanistic aspects of reaction 1.

$$M{-}NR_2 + CO_2 \rightleftharpoons M{-}O{-}\overset{\overset{O}{\|}}{C}{-}NR_2 \qquad (1)$$

$$R_2NH + CO_2 \overset{\text{fast}}{\rightleftharpoons} R_2N\overset{\overset{O}{\|}}{C}{-}OH \qquad (2)$$

$$R_2NCOOH + L_nMNR_2 \rightleftharpoons L_nM\overset{\overset{O}{\|}}{O}C{-}NR_2 + R_2NH \qquad (3)$$

The most informative mechanistic study of an authentic carbon dioxide insertion process involving a metal amide derivative is that provided by Hartwig, Bergman, and Anderson.[11] This report overcame the problem arising from the intervention of free amine by affixing the amido ligand to the

(1) Mcghee, W. D.; Riley, D. P.; Christ, M. E.; Christ, K. M. *Organometallics* **1993**, *12*, 1429.
(2) Fournier, J.; Bruneau, C.; Dixneuf, P. H.; Lécolier, S. *J. Org. Chem.* **1991**, *56*, 4456.
(3) Mcghee, W. D.; Riley, D. P. *Organometallics* **1992**, *11*, 900.
(4) Lundqvist, T.; Schneider, G. *J. Biol. Chem.* **1991**, *266*, 12604.
(5) Cleland, W. W.; Andrews, T. J.; Gtteridge, S.; Hartman, F. C.; Lorimer, G. H. *Chem. Rev.* **1998**, *98*, 549.
(6) Lynen, F.; Knappe, J.; Lorch, E.; Juetting, G.; Ringelmann, E. *Angew. Chem.* **1959**, *71*, 485.
(7) Caudle, M. T.; Kampf, J. W. *Inorg. Chem.* **1999**, *38*, 5474 and references therein.
(8) Pearson, M. A.; Schaller, R. A.; Michel, L. O.; Karplus, P. A.; Hausinger, R. P. *Biochemistry* **1998**, *37*, 6214.
(9) Chisholm, M. H.; Extine, M. W. *J. Am. Chem. Soc.* **1977**, *99*, 782.
(10) Chisholm, M. H.; Extine, M. W. *J. Am. Chem. Soc.* **1977**, *99*, 792.
(11) Hartwig, J. F.; Bergman, R. G.; Anderson, R. A. *J. Am. Chem. Soc.* **1991**, *113*, 6499.

10.1021/ic001006s CCC: $20.00 © 2001 American Chemical Society
Published on Web 02/10/2001

Scheme 1

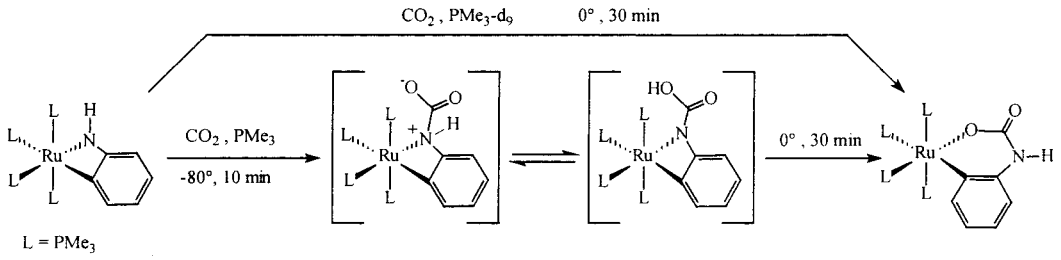

$$trans\text{-}(Cy_3P)_2Pt(Ph)NH_2 \xrightarrow{CO_2} trans\text{-}(Cy_3P)_2Pt(Ph)\underset{\displaystyle CO_2H}{\underset{|}{N}}H \longrightarrow trans\text{-}(Cy_3P)_2Pt(Ph)OC(O)NH_2 \qquad (4)$$

metal center by chelation via a strong metal−carbon bond. Specifically, the system investigated is provided in Scheme 1 with a summary of the mechanistic aspects revealed. Similarly, Roundhill and co-workers have described the formation of a N-bonded carbamate from the reaction of a platinum amide derivative and CO_2, which subsequently undergoes rearrangement to the more stable O-bonded carbamate complex (reaction 4).[12]

As expected, the pathway for CO_2 insertion into a metal-amide bond bears a close resemblance to the more widely examined reaction of CO_2 with M−OH or M−OR bonds.[13] Indeed, in the instance of carbon dioxide insertion into the M−OH bond, a pivotal step in the action of carbonic anhydrase, following the initial attack of the electrophilic CO_2 molecule at the lone pair on the metal bound hydroxide ligand formation of the bicarbonate can occur via a simple proton transfer. This has been shown not to be the case for model zinc complexes for the active site in carbonic anhydrase, where oxygen exchange between CO_2 and $H_2{}^{17}O$ was noted.[14] However, the absence of metal−oxygen bond cleavage has been noted in other systems.[15,16]

Herein, we wish to present organometallic chemistry relevant to the carbon dioxide insertion reaction involving the W−N bond of the anion $W(CO)_4$(2-amidopyridine)$^-$. Ab initio calculations on complexes and possible intermediates involved in this process will also be presented.

Experimental Section

Methods and Materials. All manipulations were performed on a double manifold Schlenk vacuum line under an atmosphere of argon or in an argon filled glovebox. Solvents were freshly distilled under nitrogen from sodium-benzophenone ketyl (tetrahydrofuran, hexane, diethyl ether), magnesium iodide (methanol), or phosphorus pentoxide followed by calcium hydride (acetonitrile). Photolysis experiments were performed using a mercury arc 450W UV immersion lamp purchased from Ace Glass Co. Routine infrared spectra were recorded on a Matteson 6022 spectrometer with DTGS and MCT detector, using a 0.10-mm CaF_2 cell. ^{1}H and ^{13}C NMR spectra were obtained on a Varian Unity+300 spectrometer and referenced to residual solvent peaks with respect to TMS. ^{13}CO and $^{13}CO_2$ were purchased from Cambridge Isotopes and were used as received. $W(CO)_6$ was purchased from Fluka and used without further purification. 2-aminopyridine (APH) and 18-crown-6 were purchased from Aldrich Chemical and used without purification. Tetraethylammonium hydroxide 25% w/w in methanol was purchased from Sigma and used as received. Microanalyses were performed by Canadian Microanalytical Service, Ltd., Delta, B. C.

Synthesis of $W(CO)_5$(2-aminopyridine), (1). 2-Aminopyridine (0.134 g) was added to 1 equiv of $W(CO)_5$THF (generated in situ by photolysis of 0.50 g of $W(CO)_6$ in 60 mL of THF for 45 min), and the solution was stirred for 30 min at ambient temperature. The product was isolated as a yellow solid upon vacuum removal of the solvent and was identified by infrared spectroscopy in the ν(CO) region. IR (THF): 2070 (w), 1926 (s), and 1897 (m). IR(MeOH): 2072 (w), 1927 (s), and 1899 (m).

Synthesis of $W(CO)_4$(2-aminopyridine), (2). Complex **2** was synthesized by photolysis of 0.50 g (1.42 mmol) of $W(CO)_6$ and 0.65 g (7.0 mmol) of 2-aminopyridine in 80 mL THF for 2 h. The solvent was then removed under vacuum leaving a yellow brown solid. The solid product was then washed with water to remove excess 2-aminopyridine, followed by washing with hexanes to remove residual $W(CO)_6$ and $W(CO)_5$(2-aminopyridine). The solid was then dried under vacuum yielding 0.38 g (68.5% yield) of a bright yellow powder. Anal. Calcd. for $[W(CO)_4(NH_2C_5H_4N)\cdot(NH_2C_5H_4N)]$ (**2**), $[C_{14}H_{12}O_4N_4W]$: C, 34.73; H, 2.50; N, 11.57. Found: C, 34.82; H, 2.54; N, 11.63. IR (CH_3-CN): 2015 (w), 1891 (s), 1875 (sh), 1831 (m). Excessive washing with water results in a significantly smaller amount of free amine present in the product as determined via ^{1}H NMR (less than ~3% free amine). IR (CH_3CN): 2011 (w), 1886 (s), 1871 (sh), 1827 (m).

Synthesis of [Na][$W(CO)_4$(2-amidopyridine)], (3). Complex **2** was deprotonated in THF solution with an excess of NaH. The yellow solution turned orange/red after a couple of hours of stirring at ambient temperature. [*If complex **2** was unwashed or only lightly washed with water prior to deprotonation, i.e., excess 2-aminopyridine was present, the reaction with NaH was instantaneous.*] The solvent was removed under vacuum to provide an orange product which was characterized by ν(CO) and ^{13}C NMR spectroscopy. IR (CH_3CN): 1988 (w), 1860 (s), 1834 (sh), 1791 (m). ^{13}C NMR **3** (CD_3CN, ppm): 207.6 $^1J_{C-W}$ = 132 Hz (2 cis COs), 214.7 $^1J_{C-W}$ = 163 Hz (1 CO trans pyridine N), 215.3 $^1J_{C-W}$ = 163 Hz (1 CO trans amido N).

Deprotonation of Complex 1, $W(CO)_5$(2-aminopyridine). Complex **1** was prepared in situ from the thermal reaction of $W(CO)_5$THF (synthesized from the photolysis of 0.50 g (1.4 mmol) of $W(CO)_6$ in THF for 45 min) and 0.13 g (1.4 mmol) of 2-aminopyridine at ambient temperature. Excess sodium hydride was added directly to the reaction solution which was stirred for 2 h resulting in an orange/red solution. The solution was filtered through Celite to provide a clear solution which contained a mixture of penta- and tetracarbonyl products, with the latter being in greater proportion. Upon cooling the solution, crystals of tetracarbonyl product (**4**) were obtained. Yellow block crystals of the pentacarbonyl product (**5**) were obtained upon addition of 18-crown-6 followed by the slow diffusion of hexanes at −20 °C. IR **4**

(12) Park, S.; Rheingold, A. L.; Roundhill, D. M. *Organometallics* **1991**, *10*, 615.
(13) (a) Darensbourg, D. J.; Sanchez, K. M.; Reibenspies, J. H.; Rheingold, A. L. *J. Am. Chem. Soc.*, **1989**, *111*, 7094. (b) Darensbourg, D. J.; Mueller, B. L.; Bischoff, C. J.; Chojnacki, S. S.; Reibenspies, J. H. *Inorg. Chem.* **1991**, *30*, 2418.
(14) Looney, A.; Han, R.; McNeil, K.; Parkin, G. *J. Am. Chem. Soc.* **1993**. *115*, 4690.
(15) (a) Chaffee, E.; Dasgupta, T. P.; Harris, G. M. *J. Am. Chem. Soc.* **1973**, *95*, 4169. (b) Palmer, D. A.; Harris, G. M. *Inorg. Chem.* **1974**, *13*, 965. (c) Buckingham, D. A. In *Biological Aspects of Inorganic Chemistry*; Dolphin, D., Ed.; John Wiley: New York, 1977; p 141.
(16) Darensbourg, D. J.; Meckfessel-Jones, M. L.; Reibenspies, J. H. *Inorg. Chem.* **1996**, *35*, 4406.

Table 1. Crystallographic Data for Complex **5**

empirical formula	$C_{16}H_{17}N_2O_8WNa$
fw	572.15
space group	*P*1(bar)
V, Å^3	990.58(11)
Z	2
d_{calc}, g/cm^3	1.922
a, Å	7.2771(5)
b, Å	10.9638(7)
c, Å	13.1279(8)
α, deg	73.9650(10)
β, deg	86.4450(10)
γ, deg	79.7780(10)
T, K	293(2)
μ(Mo Kα), mm^{-1}	5.898
wavelength, Å	0.710 73
R_F,[a] %	2.13
R_{wF},[b] %	5.24

[a] $R_F = \sum F_o - F_c/\sum F_o$. [b] $R_{wF} = \{[\sum w(F_o^2 - F_c^2)^2]/(\sum wF_o^2)\}^{1/2}$.

(CH_3CN): 1987 (w), 1863 (b), 1806 (m). IR **5** (CH_3CN): 2071 (w), 1916 (s), 1859 (m).

Reaction of [Na][W(CO)$_4$(2-amidopyridine)], 3, with CO$_2$. In a typical reaction, 0.15 g of **3** was dissolved in 15 mL CH_3CN. Gaseous done dry carbon dioxide was condensed by liquid nitrogen in a sealed flask. The CO_2 was allowed to warm slowly and was transferred via cannula into the solution of **3**. Upon addition of the CO_2, the orange solution of **3** became cloudy and slightly more yellow. The product (**6**) was characterized in solution by ν(CO) infrared and ^{13}C NMR spectroscopies. IR (CH_3CN): 2005 (w), 1881 (s), 1859 (sh), 1811 (m). ^{13}C NMR (CD_3CN, ppm): 206.9 $^1J_{C-W} = 132$ Hz (2 cis COs), 214.1 $^1J_{C-W} = 162$ Hz (1 CO trans N), 214.4 $^1J_{C-W} = 172.4$ Hz (1 CO trans O).

X-ray Crystallographic Study of Complex 5. Crystal data and details of data collection for **5** are given in Table 1. A yellow block of **5** was mounted on a glass fiber with epoxy cement at room temperature. Preliminary examination and data collection were performed on a Bruker CCD X-ray diffractometer (Mo Kα, $\lambda = 0.71073$ Å radiation) for **5**. Cell parameters were calculated from the least-squares fitting of the setting angles for 24 reflections. ω-Scans for several intense reflections indicated acceptable crystal quality. Data were collected for $1.61 \le 2\theta \le 27.50°$. Three control reflections, collected every 97 reflections, showed no significant trends. Background measurements by stationary-crystal and stationary-counter techniques were taken at the beginning and end of each scan for half the total scan time. Lorentz and polarization corrections were applied to 11 727 reflections for **5**. A semiempirical absorption correction was applied to **5**. A total of 4498 unique reflections, with $|I| \ge 2.0\sigma(I)$, was used in further calculations. The structure of **5** was solved by direct methods [SHELXS programs package, Sheldrick (1993)]. Full-matrix least-squares anisotropic refinement for all non-hydrogen atoms yielded and $R = 0.0213$, $R_w = 0.0524$ and $S = 1.214$ for **5**. Hydrogen atoms were placed in idealized positions with isotropic thermal parameters fixed at 1.5× that of the adjacent atom. Neutral-atom scattering factors and anomalous scattering correction terms were taken from the International Tables for X-ray Crystallography.

X-ray Crystallographic Study of [Na]$_2$[W(CO)$_4$(2-amidopyridine)]$_2$, (4). A preliminary data set was collected on complex **4**. An orange needle of **4** was mounted on a glass fiber with epoxy cement at room temperature. The data were collected on a Siemens P4 X-ray diffractometer (Mo Kα, $\lambda = 0.71073$ Å radiation). However, the structure could not be accurately solved as only half of the data were collected. Nevertheless, the atom connectivity was apparent.

Computational Methods. Theoretical calculations were performed using the Gaussian 94 program package employing the LANL2DZ basis set of Hay and Wadt[17] as implemented in Gaussian 94.[18] Hartree−Fock (HF) and Density Functional (DFT) calculations were carried out on the 2-aminopyridine complexes. DFT calculations were performed using Becke's three parameter hybrid method[19,20] coupled to the correlation functional of Lee, Yang, and Parr (B3LYP).[21] Full geometry optimizations were performed on all complexes starting from structures drawn using the Cerius program. Frequency calculations were also performed on **3** and **6** in order to establish the nature of the extrema and to calculate values for ΔH and ΔG. Both complexes were found to have no negative frequencies.

Table 2. IR Data for Complexes **1**−**6** in CH_3CN, Parentheses in CH_3OH

complex	IR ν(CO) cm^{-1}			
W(CO)$_5$2APH **(1)**[a]	2070(w) (2072(w))	1926(s) (1927(s))	1897(m) (1899(m))	
W(CO)$_4$2APH **(2-xs)**[b]	2015(w)	1891(s)	1875(sh)	1831(m)
W(CO)$_4$2APH **(2)**[c]	2011(w)	1886(s)	1871(sh)	1827(m)
[Na][W(CO)$_4$2AP] **(3-xs)**[b]	1988(w)	1860(s)	1834(sh)	1791(m)
[Na][W(CO)$_4$2AP] **(3)**[c]	1988(w)	1860(s)	1836(sh)	1787(m)
[Na]$_2$[W(CO)$_4$2AP]$_2$ **(4)**	1987(w)	1863(b)	1806(m)	
[Na][W(CO)$_5$2AP] **(5)**[c]	2071(w)	1916(s)	1859(m)	
[Na][W(CO)$_4$OC(O)2AP] **(6)**	2005(w)	1881(s)	1859(sh)	1811(m)

[a] In THF. [b] 5-Fold excess 2APH. [c] Excess 2APH removed.

Results and Discussion

Synthesis of the tungsten pentacarbonyl 2-aminopyridine complex (**1**) was achieved via the labile ligand displacement of THF by 1 equiv of 2-aminopyridine from the in situ photochemically generated W(CO)$_5$THF species. The infrared spectra in the ν(CO) region of **1** in THF and in methanol are quite similar (see Table 2), which is indicative of the 2-aminopyridine ligand binding to the tungsten center through the pyridine nitrogen. That is, we have previously demonstrated that binding by way of a primary or secondary amine to a {M(CO)$_5$} unit leads to a significant shift to higher frequencies of the ν(CO) vibrations in the presence of hydrogen-bonding solvents such as methanol.[21] This conclusion is reinforced upon deprotonation of complex **1** with NaH where the pyridine bond tungsten pentacarbonyl anion has been isolated and definitively characterized as its 18-crown-6 encapsulated sodium salt, **5**, by X-ray crystallography. Indeed, if in complex **5** the amido nitrogen atom was the site of ligand binding to the W(CO)$_5$ moiety, instantaneous ring-closure to form the chelated anion **3**$^-$ would have been anticipated based on the CO-labilizing ability of a π-donating amido ligand.[22−25]

On the other hand, the photolysis of W(CO)$_6$ in THF in the presence of a large excess of 2-aminopyridine provides the chelated metal derivative, W(CO)$_4$(2APH) (**2**), in good yield. Alternatively, complex **2** can be prepared by the thermal reaction of W(CO)$_6$ and 2-aminopyridine in refluxing decahydronaphthalene in low yield. Unfortunately, complex **2** is isolated with one equivalent of free ligand, i.e., as W(CO)$_4$(2APH)·2APH,

(17) Hay, J. P.; Wadt, W. R. *J. Chem. Phys.* **1985**, *82*, 284−298.
(18) Frisch, M. J.; Trucks, G. W.; Schlegel. H. B.; Gill, P. M. W.; Johnson, B. G.; Robb, M. A.; Cheeseman, J. R.; Keith T.; Petersson, G. A.; Montgomery, J. A.; Raghavachari, K.; Al-Laham, M. A.; Zakrzewski, V. G.; Ortiz, J. V.; Foresman, J. B.; Cioslowski, J.; Stefanov, B. B.; Nanayakkara, A.; Challacombe, M.; Peng, C. Y.; Ayala, P. Y.; Chen, W.; Wong, M. W.; Andres, J. L.; Replogle, E. S.; Gomperts, R.; Martin, R. L.; Fox, D. J.; Binkley, J. S.; Defrees, D. J.; Baker, J.; Stewart, J. P.; Head-Gordon, M.; Gonzalez, C.; Pople, J. A. *Gaussian 94,* revision D.4; Gaussian, Inc.: Pittsburgh, PA, 1995.
(19) (a) Becke, A. D.; *Phys. Rev. A* **1988**, *38*, 3098. (b) Becke, A. D. *J. Chem. Phys.* **1993**, *98*, 5648−5652.
(20) Lee, C.; Yang, W.; Parr, R. G. *Phys. Rev. B* **1988**, *37*, 785.
(21) Darensbourg, D. J.; Ewen, J. A. *Inorg. Chem.* **1981**, *20*, 4168.
(22) Caulton, K. G. *New J. Chem.* **1994**, *18*, 25.
(23) Poulton, J. T.; Folting, K.; Streib, W. E.; Caulton, K. G. *Inorg. Chem.* **1992**, *31*, 3190.
(24) (a) Darensbourg, D. J.; Klausmeyer, K. K.; Reibenspies, J. H. *Inorg. Chem.* **1996**, *35*, 1535 (b) Darensbourg, D. J.; Atnip, E. V.; Klausmeyer, K. K.; Reibenspies, J. H. *Inorg. Chem.* **1994**, *33*, 5230.
(25) Lichtenberger, D. L.; Brown, T. L *J. Am. Chem. Soc.* **1978**, *100*, 366.

Scheme 2

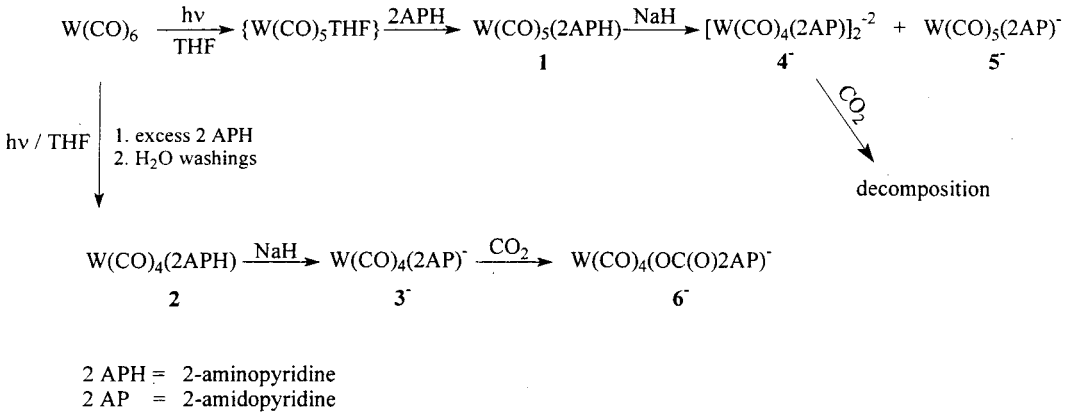

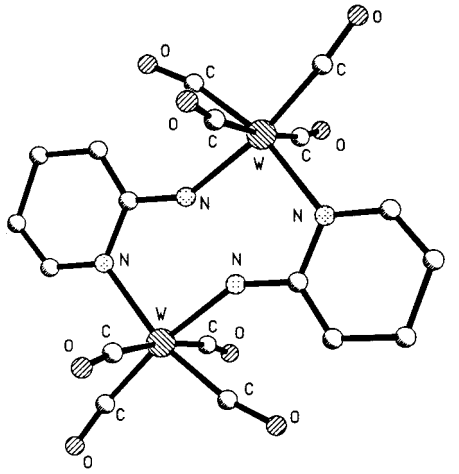

Figure 1. Ball-and-stick drawing of the dimer $[Na]_2[W(CO)_4(2AP)]_2$ (**4**) as obtained from a preliminary crystal structure.

as indicated by ^{1}H NMR and elemental analysis. Presumably, the added equivalent of 2-aminopyridine is hydrogen bonded to the complex, for upon its removal (<3%) by excessive washing with water, the ν(CO) vibrations shift on the average by 4 cm^{-1} to lower frequencies. Deprotonation of complex **2** with NaH readily takes place with formation of the amido analogue, [Na][W(CO)$_4$(2AP)], (**3**). In the presence of excess ligand, 2-aminopyridine, deprotonation occurs much more quickly, likely via the intermediacy of the deprotonated free amine, $NHC_5H_4N^-$. Complex **3** in CH_3CN rapidly reacts with carbon dioxide at ambient temperature and atmospheric pressure to yield the chelated carbamate derivative, **6** (vide infra). By way of contrast deprotonation of the pentacarbonyl tungsten derivative, complex **1**, by NaH leads to two interesting products, a tetracarbonyl dimeric derivative **4** and a pentacarbonyl derivative **5**. Complex **4**, unlike **2**, does not lead to carbamate formation in the presence of carbon dioxide, instead it undergoes a decomposition process. Scheme 2 summarizes the reactions described herein.

A preliminary crystal structure of complex **4**, $[Na]_2[W(CO)_4(2AP)]_2$, reveals it to be dimeric as shown in the ball-and-stick drawing represented in Figure 1. Unfortunately, the crystal decayed before we could obtain a complete data set, and thusfar we have been unable to obtain suitable crystals to pursue a more accurate structure determination. However, X-ray quality crystals of the other product resulting from the deprotonation of complexes **1** and **5** were obtained as the 18-crown-6 encapsulated sodium salt. Complex **5** has been characterized in the solid-state by X-ray crystallography, and a list of selected bond lengths and angles is provided in Table 3. The structure of the anion consists of a tungsten center in an octahedral environment with five carbonyl ligands and the sixth site being occupied by the pyridine nitrogen of the 2-amidopyridine ligand, Figure 2. The tungsten−nitrogen bond distance of 2.292(3) is slightly longer than the analogous tungsten−nitrogen bond in W(CO)$_5$(pyridine) of 2.26(1) Å[26,27] as well as the W−N bond in W(CO)$_5$(uracilate)$^-$

Table 3. Selected Bond Lengths [Å] and Angles [deg] for **5**[a]

W1−C1	1.980(4)	N1−C10	1.377(5)
W1−C5	2.032(5)	N2−C6	1.354(6)
W1−C4	2.045(4)	N2−Na1	2.823(5)
W1−C3	2.047(5)	Na1−O3A	2.811(4)
W1−C2	2.053(4)	Na1−O1A	2.903(4)
W1−N1	2.292(3)	Na1−Na1	3.372(7)
N1−C6	1.349(5)		
C1−W1−C5	87.55(17)	C3−W1−C2	95.28(16)
C1−W1−C4	87.39(17)	C1−W1−N1	176.62(15)
C5−W1−C4	87.88(17)	C5−W1−N1	89.24(15)
C1−W1−C3	90.34(17)	C4−W1−N1	91.42(14)
C5−W1−C3	175.94(16)	C3−W1−N1	92.79(14)
C4−W1−C3	88.56(16)	C2−W1−N1	94.45(15)
C1−W1−C2	86.52(17)	C6−N1−W1	124.7(3)
C5−W1−C2	88.06(17)	C10−N1−W1	118.4(3)
C4−W1−C2	172.81(16)	N1−C6−N2	119.8(4)

[a] Estimated standard deviations are given in parentheses.

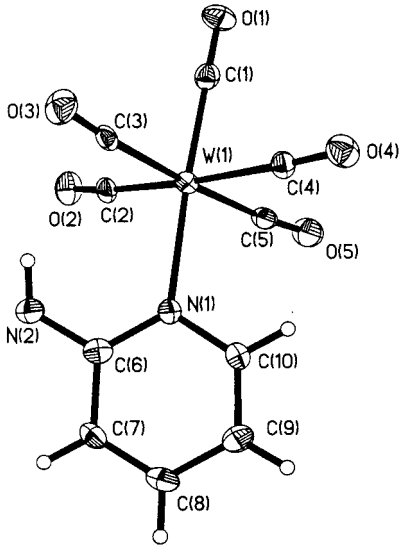

Figure 2. Thermal ellipsoid drawing of the anion of complex **5**, along with the atomic numbering scheme.

(26) Klement, U. *Z. Kristallogr.* **1993**, *208*, 111.

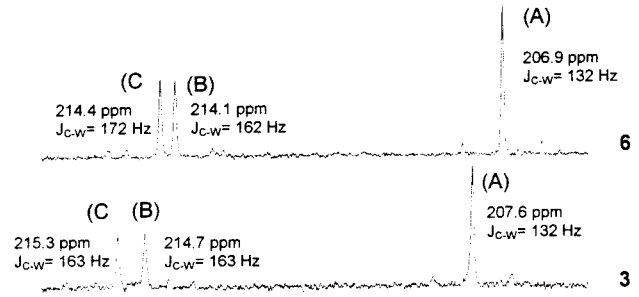

Figure 3. ^{13}C NMR spectra for complexes **3** and **6** in CH_3CN: (A) the peak due to the carbonyls cis to the nitrogens; (B) the peaks corresponding to the carbonyl trans to the pyridine nitrogen; and (C) the carbonyl trans to the amido nitrogen, the site of CO_2 insertion.

(2.281(8) Å).[28] The W−N bond here is, however, slightly shorter than the corresponding W−N bond in $W(CO)_5$(piperidine) (2.331(5) Å).[29] The CO trans to the nitrogen ligand has a carbon−tungsten bond length of 1.980(4) Å, slightly shorter than the four cis CO ligands which have W−C bond lengths which average 2.044(5) Å. The amido group on the 2-position of the ring displays interactions with a sodium cation, with a N···Na separation of 2.823(5) Å. Interestingly, two sodium ions are located within the 18-crown-6 with a $W(CO)_5(2AP)^-$ group on either side of the 18-crown-6. A representation of **5** showing the interactions between the amido nitrogens and the sodium cations is contained in the Supporting Information section.

The putative insertion reaction of CO_2 into the W−amido bond of complex **3** has been investigated by ^{13}C NMR spectroscopy. Figure 3 depicts the ^{13}C NMR spectra of **3** and the product of CO_2 insertion, **6**. As expected upon replacing an electron-rich amido ligand with a carbamate ligand the ^{13}C chemical shifts of the carbonyl ligands are displaced to lower frequency. This is consistent with the ν(CO) infrared where the frequencies shift to higher energy, an average of 21 cm^{-1}, on going from complex **3** → **6** (see Table 2). The assignment of the most high-frequency resonance in **3** at 215.3 ppm to that of the CO ligands trans to the amido group is substantiated by its $J_{^{13}C-^{183}W}$ coupling constant which undergoes a significant change upon CO_2 insertion. Concomitantly, the ^{13}C resonances due to the other three carbonyl ligands are essentially unchanged. The insertion reaction was also monitored at low temperature using ^{13}C-labeled CO_2. That is, $^{13}CO_2$ was added to a solution of complex **3** in toluene-d_8/THF at −60 °C, where a broad peak at 166 ppm along with several sharp signals at 160.8, 158.8, and 158.2 ppm were observed. Upon warming the solution to 0 °C, only a resonance at 160.8 ppm was noted which shifted to higher frequency at 162.6 ppm with further warming of the solution to 60 °C. These latter ^{13}C resonances are assigned to the carbamate ligand. It is possible that two of the other signals observed at low temperature are due to CO_2 interaction with nitrogen, i.e., $HNCO_2$ or NCOOH intermediates, as reported by Bergman, et al.[11]

In an effort to assess the relative stabilities of the various complexes investigated herein, as well as possible intermediates along the CO_2 insertion pathway, Hartee-Fock and DFT calculations were performed. Initially geometry optimizations were carried out on complex **1**, $W(CO)_5$(2APH), and its alternative amino-bound isomers (**1a**). Figure 4 contains ball-and-stick representations of complexes **1** and **1a**, along with some relevant bond distances and angles. Consistent with the experimental observations, on the basis of the energy difference between the two HF optimized isomers, **1** is more stable than **1a** by 29.4 kJ/mol. Furthermore, both isomers are thermodynamically favored over the chelated tetracarbonyl species and CO, complex **2**, by 98.5 and 69.1 kJ/mol, respectively. This is illustrated schematically in Figure 5, where the optimized geometry of complex **2** is contained in the Supporting Information.

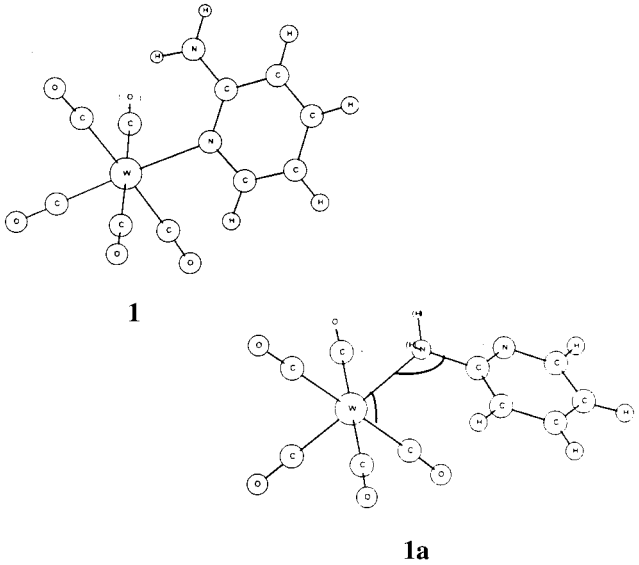

Figure 4. Ball-and-stick representations of complexes **1** and **1a** with selected bond lengths and angles shown.

Similarly, the pentacarbonyl tungsten derivatives of the deprotonated forms of **1** and **1a**, i.e., **5** and **5a**, are more stable than the chelated tetracarbonyl anion ($\mathbf{3}^-$) plus free CO. However, as might be anticipated based on the strong binding affinity of the amido ligand, isomer **5a** is slightly more stable than **5** by 10 kJ/mol. *Recall that complex **5** was synthesized by deprotonation of **1** and is probably the kinetic product.* The energy profile for this ring-closure process is depicted in Figure 6, with the optimized structure of $\mathbf{3}^-$ tabulated in Table 4. Computations were also performed on the product of CO_2 insertion into the tungsten-amido bond of $\mathbf{3}^-$. Figure 7 provides the energy profile for this insertion process where complex $\mathbf{3}^- + \mathbf{CO_2}$ is found to be less stable than either of the two isomers resulting from CO_2 insertion. The optimized structures of the two isomers, i.e., $\mathbf{6}^-$ which contains a chelated carbamate (−O−C(O)-NH− functionality) or the isomer **6a** where the hydrogen has migrated to the distal oxygen atom (−O−C(OH)═N− functionality), are supplied in the Supporting Information. As is evident from Figure 7, the more stable isomer, complex $\mathbf{6}^-$, is favored over $\mathbf{3}^- + \mathbf{CO_2}$ by −142.5 kJ/mol (HF) or −116.1 kJ/mol (DFT). Thusfar we have not been able to locate energy minima corresponding to the intermediates illustrating CO_2 interaction at nitrogen prior to CO_2 insertion into the W−N bond. We are continuing efforts to observe these reaction intermediates both experimentally and by computational methods.

Concluding Remarks

The bidentate ligand, 2-aminopyridine, has been utilized as an easily accessible starting reagent for the synthesis of a stable tungsten(0) amido complex for use in the investigation of CO_2 insertion reactions into metal-nitrogen bonds. The labile ligand substitution reaction of $W(CO)_5$THF with 2-aminopyridine

(27) Tutt, L.; Zink, J. I. *J. Am. Chem. Soc.* **1986**, *108*, 5830.
(28) Darensbourg, D. J.; Draper, J. D.; Larkins, D. L.; Frost, B. J.; Reibenspies, J. H. *Inorg. Chem.* **1998**, *37*, 2538.
(29) Moralejo, C.; Langford, C. H.; Bird, P. H. *Can. J. Chem.* **1991**, *69*, 2033.

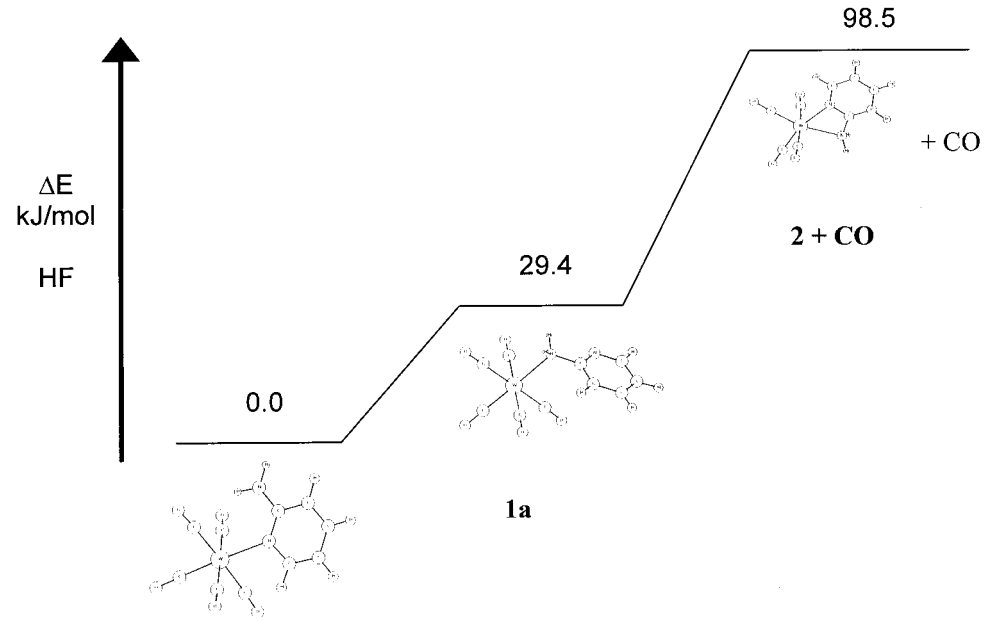

Figure 5. Calculated energy diagram of complexes **1**, **1a**, and **2** + **CO** at the HF level, energies are in kJ/mol.

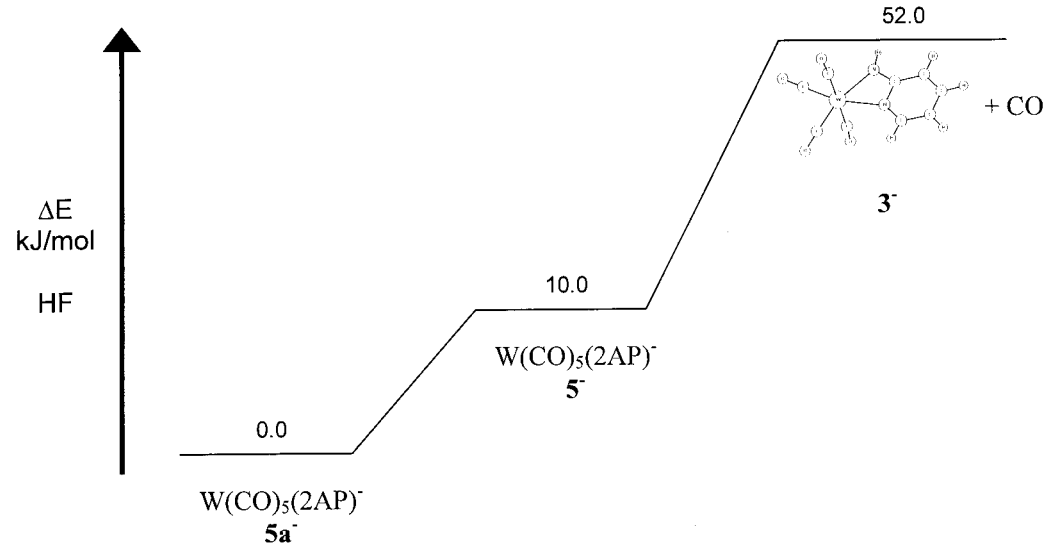

Figure 6. Calculated energy diagram of complexes **5a**$^-$, **5**$^-$, and **3**$^-$ + **CO** at the HF level, energies are in kJ/mol.

Table 4. Comparison of Selected HF and DFT Bond Lengths (Å) and Angles (deg) in **3**$^-$

bond distance/angle	HF	B3LYP
$W-N_{pyr}$	2.303	2.261
$W-N_{amido}$	2.276	2.240
$W-C_{ax}$	2.050	2.025
$W-C_{eq}$	1.971	1.966
N−W−N	57.6	59.1
$C_{ax}-W-N_{pyr}$	90.9	92.8
$C_{ax}-W-N_{amido}$	90.6	93.1
$C_{eq}-W-N_{pyr}$	104.5	103.4
$C_{eq}-W-N_{amido}$	162.1	162.5

preferentially affords the pyridine adduct, which is evidently both the kinetic and thermodynamic favored pentacarbonyl derivative. This is in agreement with ab initio computations which place the pyridine adduct some 29 kJ/mol more stable than the corresponding amine derivative. However, as might be anticipated the deprotonated ligand, $^-NHC_5H_4N$, is predicted based on computations to form the more stable derivative via the amido donor group. Nevertheless, either form of the pentacarbonyl tungsten complex can ultimately lead to the chelated anionic derivative, $W(CO)_4(NHC_5H_4N)^-$. This latter species has been found to undergo a rapid reaction with carbon dioxide to provide the carbamate complex, $W(CO)_4(OC(O)NHC_5H_4N)^-$. Concomitant ab initio computations have shown this latter six membered chelated carbamato derivative to be considerably more stable than the parent four membered chelated amido complex plus carbon dioxide. Although there are several ^{13}C resonances in the carbamate region of the ^{13}C NMR spectra taken at low temperature while monitoring the CO_2 insertion reaction, we have not been able to assign these to specific intermediates, nor have we been able to locate energy minima corresponding to CO_2 interaction with the nitrogen center prior to formation of the insertion process by computational methods. Others have postulated such intermediates based on infrared and/or NMR spectroscopic data.[11,12] Notwithstanding, we do not find our negative results surprising, for in closely related studies involving CO_2 insertion into metal alkoxides we have not found intermediates via low temperature in situ infrared spectroscopy, instead the process rapidly leads directly to metal-alkyl carbonates at −78 °C. At the same time comparative studies of CO_2

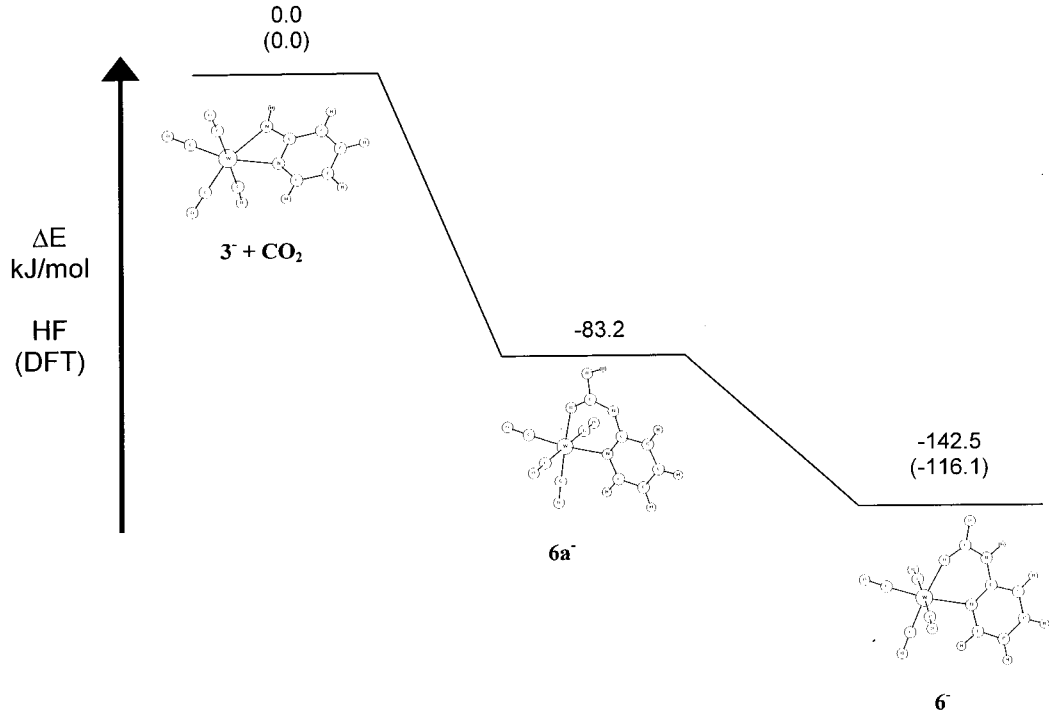

Figure 7. Calculated energy diagram of complexes $\mathbf{3}^- + \mathbf{CO_2}$, $\mathbf{6a}^-$, and $\mathbf{6}^-$ at the HF level, energies are in kJ/mol.

insertion into W−C, W−N, and W−O bonds have suggested the more nucleophile amidonitrogen to be the more reactive site.[30]

Of course there are many dialkylcarbamoto complexes synthesized from the reaction of metal chlorides with CO_2 and NHR_2; these derivatives are formed as a result of a ligand substitution process as opposed to CO_2 insertion.[31] Indeed, as has been elegantly demonstrated by Chisholm, this is a mechanistic stumbling block for assessing the precise route of metal carbamate formation from the reaction of CO_2 with metal amide.[9,10] In the case reported upon herein trace quantities of free amine were present, hence, we cannot rule out the involvement of the processes defined in eqs 2 and 3. Although a chelating amido derivative was employed in this investigation for added stability, the amido group was not strongly tethered as in the pivotal Bergman study.[11] Hopefully, the arduous task of independently determining the kinetic parameters for the various processes, i.e., reaction analogous to those in eqs 2 and 3 and the CO_2 reaction shown in Scheme 2, will be able to definitively answer this question.

Acknowledgment. Financial support from the National Science Foundation (CHE 99-10342 and CHE 98-07975 for the purchase of X-ray equipment) and the Robert A. Welch Foundation is greatly appreciated.

Supporting Information Available: X-ray crystallographic files in CIF format for the structure determination of **5** and a figure showing the interactions between amido nitrogens and the sodium cations; Optimized geometries of complexes **2**, $\mathbf{6}^-$, and **6a**. This material is available free of charge via the Internet at http://pubs.acs.org.

IC001006S

(30) Legzdins, P.; Rettig, S. J.; Ross, K. J. *Organometallics* **1994**, *13*, 569.
(31) Arimondo, P. B.; Calderazzo, F.; Englert, U.; Maichle-Mössmer, C.; Pampaloni, G.; Strähle, J. *J. Chem. Soc., Dalton Trans.* **1996**, 311.